Biophysical Chemistry 182 (2013) 23–29

Contents lists available at ScienceDirect

Biophysical Chemistry

journal homepage: http://www.elsevier.com/locate/biophyschem

Different effects of Alzheimer's peptide Aβ(1–40) oligomers and fibrils on supported lipid membranes

Claudio Canale [a], Silvia Seghezza [a], Silvia Vilasi [b], Rita Carrotta [b,*], Donatella Bulone [b], Alberto Diaspro [a], Pier Luigi San Biagio [b], Silvia Dante [a,c]

[a] Nanophysics, Istituto Italiano di Tecnologia, Via Morego 30, 16163 Genova, Italy
[b] Institute of Biophysics, CNR, Via Ugo La Malfa 153, 90146 Palermo, Italy
[c] Neuroscience and Brain Technologies, Istituto Italiano di Tecnologia, Via Morego 30, 16163 Genova, Italy

HIGHLIGHTS

- The supported lipid bilayer is a membrane model system sensitive to Aβ aggregates.
- The approach allows to point on interaction effects without any aggregation.
- Aβ oligomers produce large holes in the double layer.

GRAPHICAL ABSTRACT

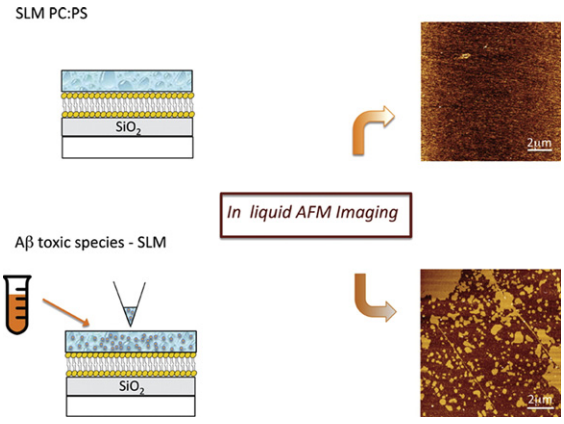

ARTICLE INFO

Article history:
Received 24 April 2013
Received in revised form 18 July 2013
Accepted 19 July 2013
Available online 14 August 2013

Keywords:
Aβ toxicity
Supported lipid bilayers
In liquid AFM
Force spectroscopy

ABSTRACT

Beta-amyloid (1–40) is one of the two most abundant species of amyloid-beta peptides present as fibrils in the extracellular senile plaques in the brain of Alzheimer's patients. Recently, the molecular aggregates constituting the early stage of fibril formation, i.e., oligomers and protofibrils, have been investigated as the main responsible for amyloid-beta cytotoxic effect. The molecular mechanism leading to neurodegeneration is still under debate, and it is common opinion that it may reside in the interaction between amyloid species and the neural membrane. In this investigation Atomic Force Microscopy and spectroscopy have been used to understand how structural (and mechanical) properties of POPC/POPS lipid bilayers, simulating the phospholipid composition and negative net charge of neuritic cell membranes, are influenced by the interaction with Aβ(1–40), in different stages of the peptide aggregation. Substantial differences in the damage caused to the lipid bilayers have been observed, confirming the toxic effect exerted especially by Aβ(1–40) prefibrillar oligomers.

1. Introduction

Alzheimer's disease (AD) is a chronic and progressive syndrome, which affects about 5% of the population over age 65. It represents the most common cause of dementia in the elderly population. From a molecular point of view, AD is characterized by the accumulation of a 39–42 amino acid peptide, the amyloid-beta peptide (Aβ), in insoluble cerebral plaques, known as amyloid fibrils [1]. The amyloid aggregation process in solution follows typical nucleation-polymerization kinetics, characterized, in each phase, by structural intermediates presenting

* Corresponding author.
E-mail address: rita.carrotta@pa.ibf.cnr.it (R. Carrotta).

0301-4622/$ – see front matter © 2013 Elsevier B.V. All rights reserved.
http://dx.doi.org/10.1016/j.bpc.2013.07.010

specific dimensions, morphologies and cytotoxic activity. Substantial evidence suggests that small, prefibrillar oligomers that form at the beginning of the aggregation path represent the most toxic amyloid species [2–4]. Experimental evidences connect the interaction between Aβ peptides and the neural membranes as the trigger of the neurotoxic mechanism [5–7]. Nevertheless, the specific molecular mechanisms underlying Aβ/membrane interaction remain to be elucidated. The reciprocal action of Aβ and membranes can be analyzed in two different perspectives. On one hand, Aβ species have been reported to damage the membrane structure [8,9] and to perturb its ionic balance [10] as well as its mechanical stability [11]. On the other hand, the membrane surface itself, depending on its chemistry, may locally act as a catalyzer for the peptide misfolding, producing dangerous intermediates and triggering the fibrillogenesis [12]: the membrane acts as a bidimensional template for the aggregation steps of the Aβ peptide. In this scenario, the use of supported lipid bilayers (SLBs), obtained through Langmuir–Blodgett deposition or through fusion of unilamellar vesicles on a flat surface [13,14], and mimicking the composition of natural neural membranes is of particular appeal in order to select and elucidate particular aspects of this interaction at a molecular level. In particular, Atomic Force Microscopy (AFM) is an ideal tool to study the effect of exogenous molecules on lipid bilayers, especially because it allows the in situ investigation in physiological conditions; AFM has therefore become a well-established technique for imaging SLBs at the nanoscope resolution and, in the spectroscopy mode, for the analysis of the membrane nanomechanics; this latter is analyzed through the acquisition of force–distance curves and the determination of the breakthrough force F_b for SLBs [15,16] and is directly related to lipid packing and lipid order in the membrane.

In this investigation we have studied the effects of different Aβ(1–40) intermediates on SLBs by AFM imaging and force spectroscopy. As model membrane, SLBs made of a mixture of 9:1 mol/mol of 1-palmitoyl-2-oleoyl-phosphatidylcholine (POPC) and 1-palmitoyl-2-oleoyl-phosphatidylserine (POPS) were used, in order to mimic, as closely as possible, the composition and the negative charge state of neuritic cell membranes without increasing the complexity of the system too much. The same lipid mixture was used in our preliminary studies showing that the interaction and intercalation of different Aβ species are very dependent on anionic state and composition of the membrane [17,18].

The different Aβ species at the various instants of the aggregation kinetics have been found to produce different effects not only on the structure but also on the mechanical properties of the SLBs. A peculiar instant of transition between membrane active and membrane-nonactive Aβ peptides has been also evidenced.

2. Materials and methods

2.1. Aβ aggregation by fluorescence spectroscopy

The synthetic peptide Aβ(1–40) (PolyPeptide Laboratories, Strasbourg, France) was pretreated according to the procedure of Fezoui et al. [19] for improving the reliability of experiments at neutral pH. Stock aliquots (200 μg each) were stored at −80 °C.

Aβ(1–40) samples were prepared by dissolving the lyophilized peptide in 50 mM phosphate buffer, pH 7.4, at a concentration of about 70 μM. The solution was serially filtered through 0.22 μm (Millex-LG) and 20 nm (Anotop-Whatman) filters into a fluorescence quartz cuvette containing a small magnetic stirring bar. Aβ(1–40) concentration was determined by tyrosine absorption at 276 nm using an extinction coefficient of 1390 cm^{-1} M^{-1} [20]. The sample was then diluted to the working Aβ(1–40)concentration of 48 μM, by adding the appropriate amount of buffer and tiny amount of a concentrated solution of Thioflavin T (ThT) to have a final ThT concentration of 12 μM.

The change in ThT fluorescence emission during the kinetics of Aβ aggregation was monitored by using a JASCO FP-6500 spectrometer.

The excitation and emission wavelengths were 450 and 485 nm, respectively and the slit width was set to 3 nm both in excitation and emission. The sample was placed in the cell compartment thermostated at 37 °C, and continuously sheared at 200 rpm by using a magnetic stirrer (mod. 300, Rank Brothers Ltd., Cambridge). Each experiment was repeated at least three times. Aliquots of 100 μL of solution were taken away at different times to be used for AFM characterization and bilayer interaction studies.

2.2. Supported lipid bilayers

The phospholipids used for vesicle preparation were the zwitterionic 1-palmitoyl-2-oleoyl-phosphatidylcholine (POPC) and the negatively charged 1-palmitoyl-2-oleoyl-phospatidylserine (POPS) from Avanti Polar Lipids (Alabaster, Alabama, US). The lipids were dissolved in chloroform/methanol (Sigma-Aldrich) 2:1, mixed in a ratio POPC/POPS 9:1 mol/mol and gently dried under a nitrogen flux. Solvent traces were removed under vacuum, overnight. The lipid mixtures were then resuspended in Phosphate Buffer Saline (PBS 1×), in a concentration of 1 mg/ml, vortexed and let to swell for at least 30 min. The resulting opalescent suspension was extruded at least 11 times through polycarbonate membranes with 100 nm pores using a commercial extruder (Avanti Polar Lipids). The obtained large unilamellar vesicles (LUVs) were then diluted 10 fold and 50 μL of the vesicle suspension was administered to the solid support for AFM investigation. Square silicon supports 5 mm × 5 mm were used as substrates; before use, the Si surface was cleaned with a sodium dodecyl sulfate (SDS) solution under sonication (30 min), rinsed with Milli-Q water several times and put in an UV/Ozone chamber (Bioforce, US) for at least 30 min to remove any organic contamination. The vesicles were let in incubation overnight at ambient temperature at high relative humidity to allow vesicle fusion and to achieve uniform lipid bilayer formation. The substrate was then gently rinsed with Milli-Q water to remove the vesicle in excess.

2.3. Aβ peptide

After imaging the lipid bilayer to acquire a topographical view of the surface and collecting force curve maps in at least 5 different areas, so to ensure homogeneity of the sample, fresh solutions of Aβ were prepared by suspending in phosphate buffer the aliquots, collected at the different stages of fibrillization. The final concentration was 1 μM. Thereafter, 40 μL of 1 μM Aβ solutions was administered to the liquid subphase in contact to the lipid bilayer and let to incubate 20 min and carefully rinsed. The sample was then placed again under the AFM for topographical inspection.

2.4. AFM imaging

All AFM measurements were performed by using a Nanowizard III (JPK Instruments, Germany) mounted on an Axio Observer D1 (Carl Zeiss, Germany) inverted optical microscope. V-shaped silicon nitride cantilevers (SNL, USA), with a nominal spring constant ranging from 0.12 N/m to 0.48 N/m, with a resonance frequency in air ranging from 40 kHz to 75 kHz and tip with typical curvature radius of 2–12 nm were used. The actual spring constant of each cantilever was determined in situ, using the thermal noise method [21].

Aliquots of protein solutions (1 μM) were deposited onto freshly cleaved mica surfaces (Agar Scientific, Assing, Italy) and incubated for up to 20 min before rinsing with deionized water and drying under a low pressure nitrogen flow. Imaging of the protein was carried out in intermittent contact mode in air.

To image the supported lipid bilayers, the silicon substrates were fixed to a glass coverslip by using a two-component epoxy glue. The samples were always kept in an aqueous subphase. AFM images were collected using Quantitative Imaging mode (QI mode, JPK), working in liquid environment. In QI mode the height information is extracted

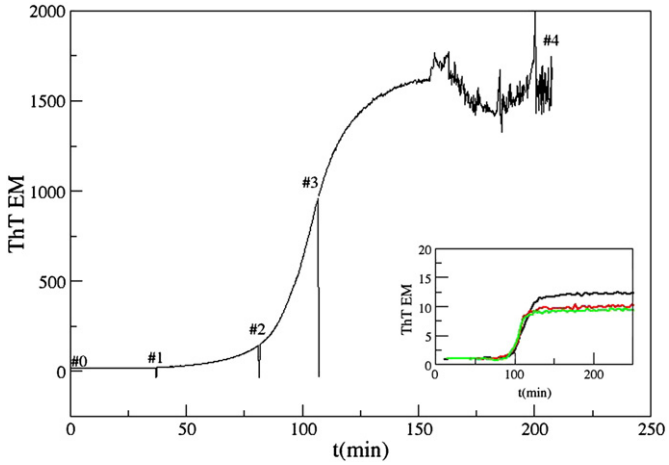

Fig. 1. Time course aggregation of a 48 μM solution of Aβ(1–40) at 37 °C, monitored by ThT fluorescence increase. The emission and excitation wavelengths were 485 and 450 nm, respectively, and 3 nm the emission and excitation slit width. ThT concentration was 12 μM. Aliquots of 100 μL of solution were taken away at different time processes, as marked by numbers in the plot. The inset reports on the kinetic data monitored in a plate reader setup. Experiments are conducted in triplicate under very similar conditions (agitation, T = 37 °C, 48 μM peptide concentration and 12 μM ThT concentration, same buffer) to the ones reported in the main panel, monitored in a spectrofluorimeter.

from a force–distance curve computed from each pixel of the image. The force curve set point was in the range of 0.4–0.8 nN, with a tip velocity of 30 μm/s.

2.5. AFM force spectroscopy

Force spectroscopy maps were acquired in contact mode. The same cantilevers used for imaging were employed. In force mapping, a sequence of force–distance curves was collected over at least 5 different areas of the supported membrane. The areas had a dimension of 10 μm × 10 μm and were divided in grids of 20 × 20 sampling points. In each point an extension–retraction force–distance curve was recorded. The applied load was in the range of 10–25 nN, the curve length was 300 nm and the tip velocity of 1 μm/s was maintained constant.

For each sample at least 5 maps consisting of 400 force–distance curves were collected and analyzed using a home built algorithm.

The maps were collected on the same SLB before and after interaction with Aβ(1–40) for each of the sampled instant of the aggregation kinetics.

3. Results and discussion

3.1. Aβ(1–40) fibrillogenesis

ThT fluorescence increase was used to monitor the fibrillization kinetics of a 48 μM Aβ(1–40) solution at 37 °C, under stirring. Samples were continuously sheared at a 200 rpm rate. ThT fluorescence of the sheared sample was measured in situ in the cuvette cell. Aliquots (t_0, t_1, t_2, t_3, t_4) were removed at chosen times and kept at 4 °C, in order to significantly slow down the self-assembling process. Freezing was avoided on purpose for preventing Aβ(1–40) solution

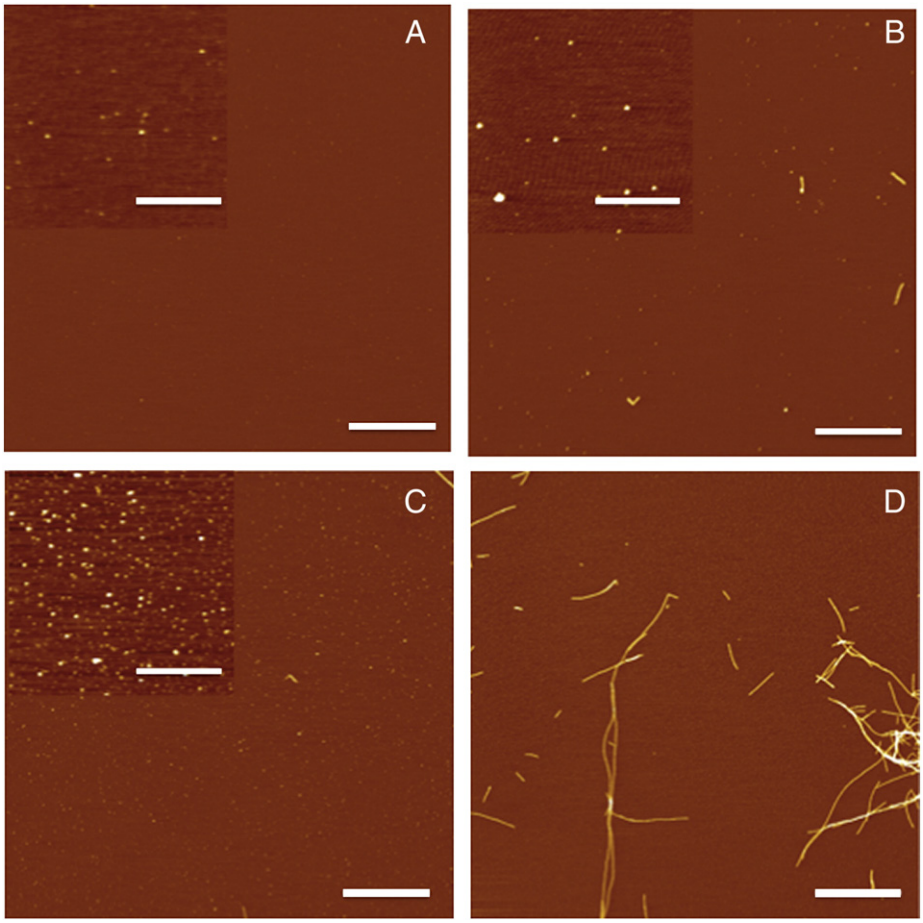

Fig. 2. AFM images of the different Aβ(1–40) intermediate species desiccated on mica at different times of the aggregation kinetics (scale bars A–D 2 μm, z-range 10 nm). As highlighted in the insets (scale bar 1 μm, z-range 2 nm) at t_0 (A) the peptide aggregates are very small, about few tens of nanometers in lateral size and in the nanometer range in thickness. Increasing the aggregation time, the dimension and surface density of the globular aggregates increase, as visible in panels B and C, corresponding to t_1 and t_2, respectively. At the final time of the kinetics (t_4, D), only fibers are detected.

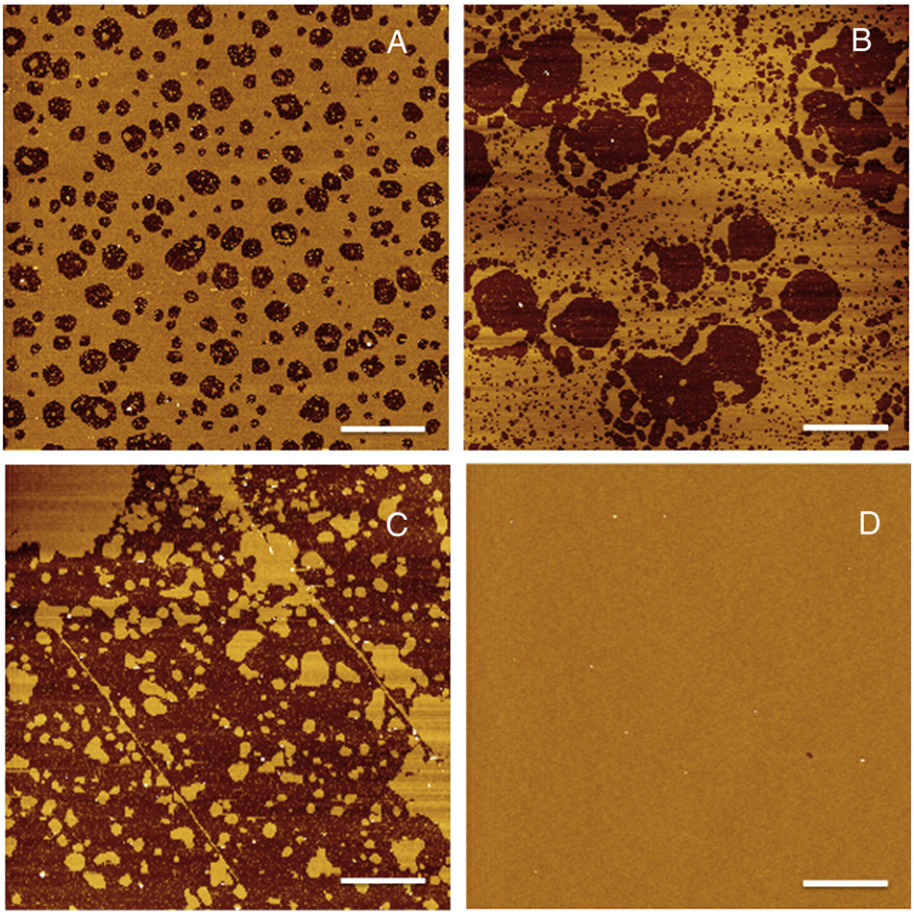

Fig. 3. Topography of POPC/POPS SLB subjected to Aβ(1–40) species sampled at different aggregation instants: at t_0 (A) many holes are detected, i.e., regions of the lipid membranes detached from the surface after interaction with Aβ; the amount of damage increases with the aggregation time of Aβ as shown in B (t_1) and C (t_2). Finally, the fibers present at t_4 do not harm the SLB (scale bars A–D 2 μm, z-range 10 nm).

from freezing–thawing cycles. The different aliquots of Aβ(1–40) were diluted to 1 μM, before deposition on mica for imaging by tapping mode AFM and for following studies on Aβ species/bilayer interaction. Fig. 1 shows the ThT signal time course during a fibrillization kinetics [22] for a solution of Aβ(1–40), under stirring conditions. The curve displays the sigmoidal behavior typical of Aβ fibrillization, characterized by a lag-phase (times t_0, t_1 and t_2) followed by a sudden cooperative increase of the signal (t_3) and exhibiting in average a final plateau (time t_4). Literature data show that small aggregates and a few small protofibrils build during the lag-phase. After that, the numbers of protofibrils increase quickly with time during the so-called elongation phase (enhanced also by stirring conditions), while some mature fibers begin to form. Fig. 1 shows an evident increase in the noise level after 150 min of incubation. The reason of the noise onset is that the sample starts to contain large and long fibrils with tendency to precipitate. These species cause fluctuations in the signal, since they can pass by the volume of observation. This regime can also be prompted and sustained by agitation which works in re-mixing the fibrils in solution. The inset in Fig. 1 reports on the Aβ(1–40) aggregation process time course, conducted in triplicate by collecting data from a plate reader setup, in order to give confidence of the repeatability of the sigmoidal behavior, under the conditions studied.

Table 1
Surface coverage of POPC/POPS SLB incubated with Aβ(1–40) corresponding to different instants of the aggregation kinetics.

Aggregation time	Surface coverage (%)
Lipid bilayer	99.5 ± 0.6
t_0 (0 min)	72 ± 2
t_1 (37.5 min)	60 ± 2
t_2 (82 min)	26 ± 3
t_3 (110 min)	11 ± 2/99 ± 1
t_4 (200 min)	98 ± 1

3.2. AFM investigation of Aβ aggregates

Aβ species at different points of the aggregation kinetics have been desiccated on mica after 20 min incubation time and imaged in air by AFM. The corresponding topographical images are summarized in Fig. 2. The 10 μm views of the samples well describe the different steps of the fibrillogenesis; in each of the steps aggregates of different size and shape are present. In the first analyzed Aβ sample, corresponding at t_0 in the kinetics curve, (Fig. 2A) very small particles are present; the enlargement in the inset of the figure shows that the dimensions of these species are about few tens of nanometers. Increasing the aggregation time in the kinetic curve larger globular aggregates 100 nm in lateral size are found (Fig. 2B and C, corresponding at t_1 and t_2, respectively), whose thickness is about 10 nm, and whose density on the surface increases notably. Mature fibrils appear in the t_4 sample only (Fig. 2D). A control experiment incubating buffer alone on mica has also been performed; the corresponding results are shown in Fig. S1 (A) in Supplemental material. In this work the AFM has been used to detect the progression of the aggregation process. The determination of an absolute value that characterizes the aggregate size was not the aim of our study, hence we did not discuss in details the different affection that influence the apparent size of small object imaged by AFM [23].

3.3. Aβ interaction with supported lipid bilayers

3.3.1. AFM imaging

Aβ samples homologous to those desiccated on mica and inspected by AFM have been administered to POPC/POPS lipid bilayers; Aβ has been let in incubation in phosphate buffer for 20 min, after administration to the lipid bilayer, and therefore gently removed and substituted with the same buffer, with special care not to dehydrate the lipid sample. The topography of the lipid bilayer was controlled by AFM before Aβ administration and only defect-free bilayer, i.e., topographically flat, was used for further investigation; an example of SLB produced after overnight vesicle incubation is shown in Fig. S1 (B) in Supplemental material. Since in most of cases SLB topography before peptide incubation does not display significant defects, the presence of a bilayer on the substrate cannot be easily proven only through imaging. For this reason, we decided to verify the actual SLB coverage by analyzing force spectroscopy data recorded overall the 100 μm × 100 μm AFM scanning area. As it will be described in details in the next section, each force curve acquired on a bilayer covered region presents a characteristic breakthrough event that is not observed in correspondence of holes, where the tip interacts directly with the substrate (Fig. 5A); thus, the percentage of curves containing a breakthrough event in the 5 sets of 400 curves acquired for each sample can be used as a measurement of SLB coverage. A surface coverage of 99.5 ± 0.6% has been determined for SLBs formed after overnight incubation, averaging the results of 13 different samples.

Fig. 3 reports the topography of the lipid bilayers after exposure to the different investigated Aβ species. Already at t_0 the bilayer appears to be heavily damaged: roundish areas in which the bilayer has been removed from the surface are uniformly distributed on the samples; at t_1 the size of the holes has considerably increased and bigger empty areas are surrounded by a great number of smaller ones. At t_2 the SLB is almost completely destroyed by the action of Aβ(1–40) and only separated islands of intact membrane are left on the surface. The surface coverage has been quantified in each of the steps and is reported in Table 1. On the contrary, when the last Aβ species, obtained at t_4, have been incubated with the SLB, the topography of the lipid bilayer appears to be unperturbed: the bilayer is uniformly flat and without holes. Control measurements, incubating the sample with pure buffer and rinsing, were carried on. In this case, no effect on the bilayer topography was observed (Fig. S1 (B–C) Supplemental material).

These results unequivocally demonstrates that Aβ(1–40) fibrils, i.e. the preponderant species at t_4, do not harm the membrane and that the oligomers or proto-fibrils present at the early stage of the aggregation path are the most dangerous forms. They actively interact with the bilayer and presumably form aggregates with the lipids, which are removed from the surface in the rinsing step.

The disruptive effect of Aβ peptides on lipid bilayers had been already reported in the literature for different Aβ peptides. For instance Aβ (1–42) at the early aggregation stage was found to heavily perturb and destabilize POPC/POPS membranes on mica or on polymeric cushion [11]; the destruction of SLB of total brain lipid extract bilayer by Aβ(1–40) and Aβ(1–28) [24] has been also reported. In that case, the peptide action was monitored over time on the SLB: patches of lipids had been displaced from the surface after 15 h incubation and were surrounded by short fibrils. This result is apparently in contradiction with our current finding, in which the fibers seem to be inactive on the membrane; the main difference between the two investigation is that Yip and McLaurin monitored the effect of fibrillogenesis of Aβ in situ in the presence of the membrane; in our case fibrillogenesis occurred separately and fibers already formed were incubated with SLBs. This finding therefore reinforces the knowledge that the interaction between Aβ and phospholipid is necessary to produce a harmful effect on the membrane. To this regard, specific membrane properties affecting protein–membrane binding and amyloid aggregation have been found also for α synuclein, an intrinsically disordered and amyloidogenic protein, which is involved in Parkinson's disease (PD) etiology [25]. Membrane-mediated protein conformational changes are linked to disease pathogenesis making the study of membrane–protein interactions of crucial importance [23].

A controversial result, which deserves a separate discussion, was obtained at the step indicated with t_3 in the kinetics. The first examined SLB after Aβ incubation showed a complete devastation of the bilayer surface. The subsequent trials, performed with other aliquots of Aβ(1–40) taken at t_3 and incubated to other POPC/POPS bilayers at subsequent time (either the same day or a few days later), resulted in perfectly unperturbed bilayers, i.e., it caused the same effect observed when using Aβ(1–40) at the last stage of fibrillogenesis. The corresponding morphologies of the Aβ samples on mica are reported in Fig. 4A and C. In the first case globular aggregates of 100 nm in lateral size are uniformly distributed on the mica surface, and also beaded chain fibers are well visible in the sample; in the second case, many fibrils several μm in length are present in the sample. We infer from these results that t_3 is a rather peculiar instant in the aggregation process, very close to a conformational transition, which can swap the morphology of the aggregates from membrane-active species to inactive ones. The parameters leading to this crucial conformational change are at the moment not clear and are the subject of further investigation. Remarkably, only the first investigated sample of the SLB replicates incubated with Aβ(1–40) at t_3, produced a disrupting effect on the bilayer, which confirms that the evolution of the aggregation process slowly advances even if the sample is kept at 4 °C and spontaneously leads to this conformational change.

Similar defects within mica supported lipid bilayers have been induced by the amyloidogenic human amylin peptide (hA). Several

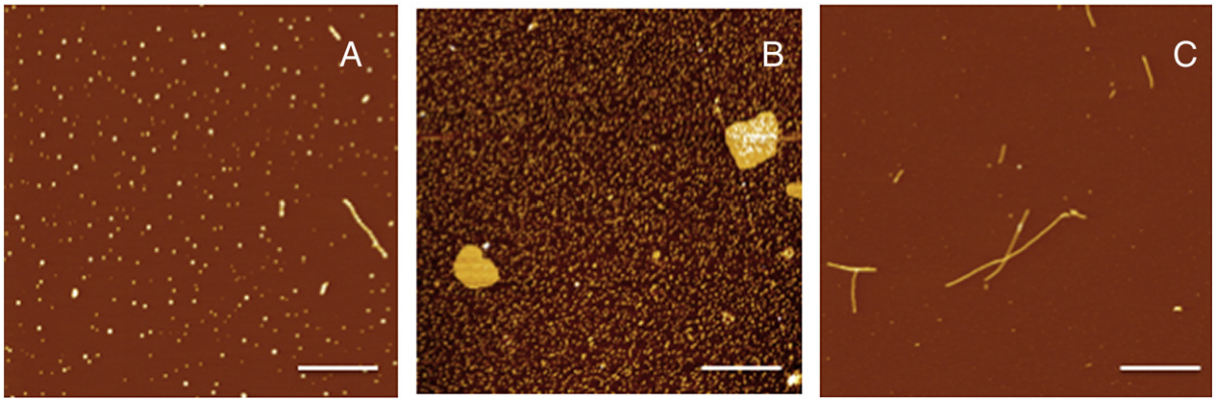

Fig. 4. Different Aβ(1–40) species desiccated on mica from different aliquots at t_3 are displayed in panels A and C. The aggregates in A produced a complete disruption of the bilayer (B); on the contrary, the elongated aggregates in B did not cause a detectable damage of the membrane (scale bars: panels A and C 2 μm, panel B 0.5 μm, z-range 10 nm).

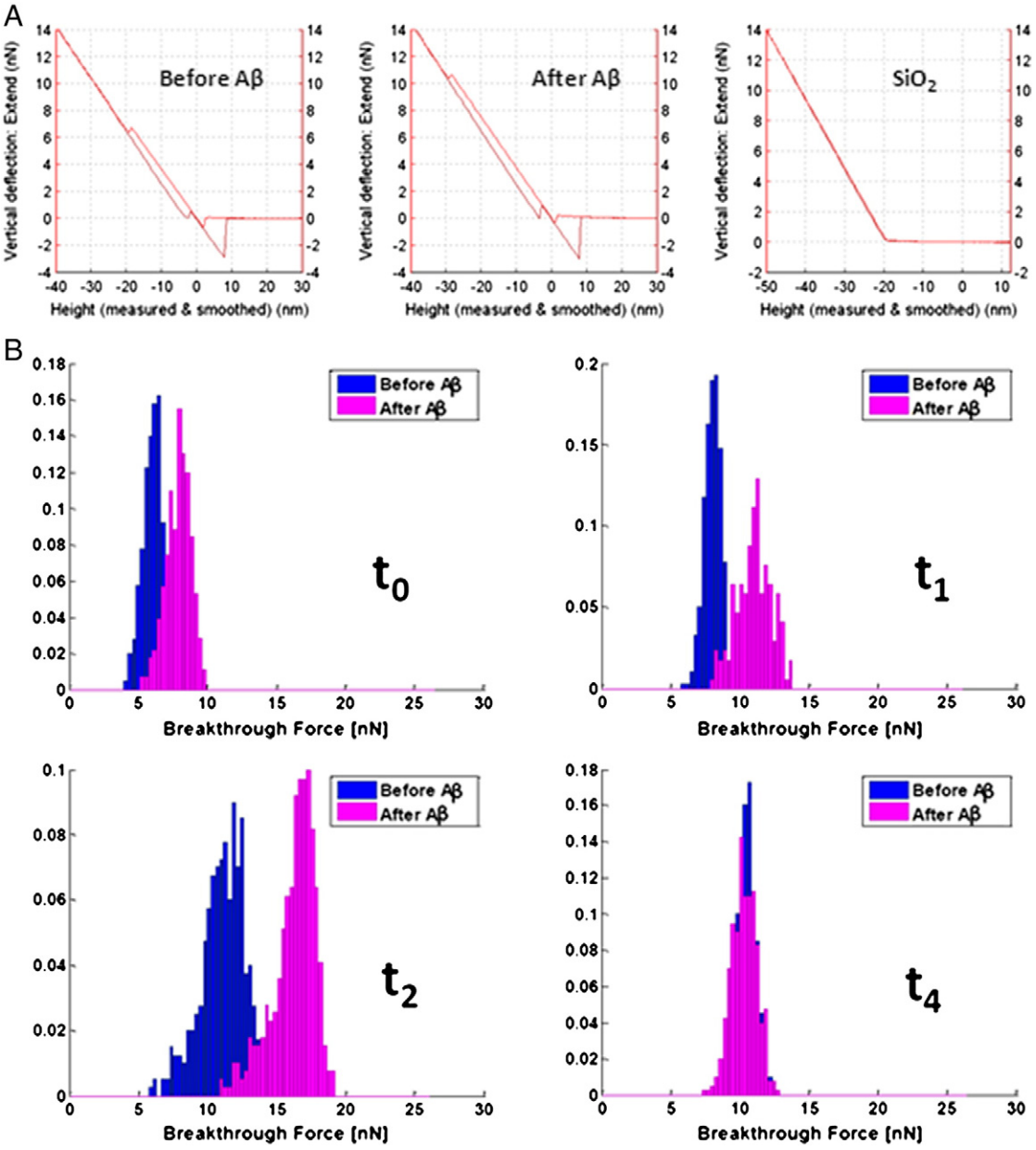

Fig. 5. A: F–d curves acquired on a POPC/POPS bilayer before and after interaction with Aβ(1–40) (example curves are taken from t_1 experiment). The curves are characterized by a typical jump-to-contact; at higher forces the breakthrough force is recorded and appears as a discontinuity in the curve. On the right, a F–d curve obtained on a silicon dioxide surface is reported. B: Histograms of the breakthrough forces measured before (blue) and after (pink) administration of the different Aβ(1–40) to the SLB in phosphate buffer. A shift of the indentation force towards higher values is observed at t_0, t_1 and t_2. On the contrary, at t_4 no significant variation of the force distributions is detected upon interaction with Aβ(1–40) fibers. To verify statistical significance, we performed ANOVA test on the 4 couple of populations depicted in the histograms: only in the t_4 experiment the two group means are not significantly different ($p < 0.05$).

mechanisms, in that case, have been hypothesized to explain the membrane lesions: loss of lipid molecules or a carpet-like mechanism similar to that previously suggested for membrane permeation by antimicrobial peptides [26]. In carpet-like mechanism, peptides initially bind to the surface of the target membrane and cover it or part of it in a carpet-like manner implying an increase of the membrane packing density by direct insertion of the peptides between lipid molecules [26].

3.3.2. AFM force spectroscopy

The mechanical properties of the SLB in the absence and in the presence of Aβ(1–40) have been investigated by AFM force spectroscopy. Force–distance (F–d) curves have been recorded on each membrane before and after exposure to Aβ(1–40). Two typical curves are displayed in Fig. 5A, along with a curve acquired on bare silicon nitride. The breakthrough event i.e., the discontinuity in the approach part of the F–d curve, is clearly visible at about 6 nN and 10 nN, before and after interaction with Aβ, respectively. The values of the breakthrough forces are well in agreement with values reported in the literature for bilayers of phospholipids with an unsaturated alkyl chain and measured in physiological ion strength conditions [27]. The comparison between the forces corresponding to the breakthrough event in the two conditions is representative of the mechanical effect induced on the membrane by the different Aβ intermediates. The results are summarized in Fig. 5B. After interacting with Aβ (pink histograms) the curve distributions are slightly right shifted in all cases, with the exception of the interaction with Aβ fibrils sampled at t_4; this result confirms that the presence of Aβ fibrils does not destabilizes the structure of the SLB and indicates a very weak Aβ fibrils/membrane interaction. When

smaller intermediates interact with the SLB, the removal of part of the bilayer evidenced by AFM imaging is unexpectedly accompanied by a rigidifying effect of the membrane on the silicon substrate. The effect is rather small at t_0, but it becomes significant at t_1 and t_2, where the force distributions, before and after interaction with Aβ, overlap only partially. This result is very different from a previous result of our group in which Aβ(1–42) was found to mechanically weaken SLB on mica and on charged polymer cushions [11]. The experiment described in the current paper differs from the previous one for several aspects: first of all, the utilized substrates (and their surface properties) were different (silicon vs. mica and polymer cushions), as well as the Aβ peptides (Aβ(1–42) vs. Aβ(1–40)) and the pretreatment used for each of them; additionally in the experiment here described we have exploited the slow kinetics of aggregation of Aβ(1–40) to separate the Aβ intermediates at different instants, reducing the variability of the system.

Moreover, it is worthy to mention that, in the current investigation, all the acquired force–distance curves are characterized by a significant jump to contact feature, which was never observed in the experiment displaying a decrease of the breakthrough force upon peptide action. This indicates once more that the interaction between membrane and Aβ may follow different paths depending on many parameters, such as the boundary conditions, the interaction with the substrate, and especially on the Aβ species present in solution. From our results it seems that small protofibrils (i.e., the intermediates present in the range of the kinetics between t_2 and t_3) could create complexes with the lipid matrix and solubilize it. On the other hand, the lipid region topographically not affected after Aβ(1–40) interaction, become mechanically more stable, such as the lipid packing would become more dense in these areas. Interestingly, the β-amyloid peptide-25–35 has been found to decrease the fluidity of mouse brain and human lymphocyte membranes, with important consequences on the membrane-associated ionic channel functions [28]. When the disruption of the lipid membrane is heavy, such as in the case of Aβ(1–40) at t_2 (Fig. 4B) and Aβ(1–42) on mica [11], the force spectroscopy data measured after peptide action are taken from lipid patches of very small size (tens to hundreds of nanometers), possibly loosely bound to the substrate, and are tremendously affected by boundary effect; it is therefore not surprising that the force distributions indicate, in those cases, a complete mechanical destabilization of the system.

4. Conclusions

The results presented here confirm the toxic action exerted by Aβ(1–40) prefibrillar oligomers, thus considered the species mainly responsible for the amyloid pathogenicity. Moreover, they contribute to attribute to the membrane damage a crucial role in the onset of disease and neuronal cell degeneration with the lipid fluidity a potential key parameter indicative of the membrane state.

In the future, a detailed analysis of force–distance curve, by the same methodological approach, performed in the presence of cholesterol, connected to AD, will further clear the role assumed by membrane rigidity in the general toxic framework. The comparison of these structural measurements to membrane–peptide interaction kinetics, by the study of leakage formation in lipid vesicles, will also be important in order to significantly improve our understanding of protein–membrane interface.

Supplementary data to this article can be found online at http://dx.doi.org/10.1016/j.bpc.2013.07.010.

Acknowledgments

This work has been partially supported by the following projects: MERIT ‘Basi molecolari nelle sindromi degenerative correlate con l’invecchiamento’; and FIRB RBFR12SIPT MIND: ‘Indagine multidisciplinare per lo sviluppo di farmaci neuro-protettori’.

References

[1] D.J. Selkoe, The molecular pathology of Alzheimer's disease, Neuron 6 (1991) 487–498.
[2] R. Kayed, A. Pensalfini, L. Margol, Y. Sokolov, F. Sarsoza, E. Head, J. Hall, C. Glabe, Annular protofibrils are a structurally and functionally distinct type of amyloid oligomer, Journal of Biological Chemistry 284 (2009) 4230–4237.
[3] R. Kayed, Y. Sokolov, B. Edmonds, T.M. McIntire, S.C. Milton, J.E. Hall, C.G. Glabe, Permeabilization of lipid bilayers is a common conformation-dependent activity of soluble amyloid oligomers in protein misfolding diseases, Journal of Biological Chemistry 279 (2004) 46363–46366.
[4] Y.V. Sokolov, R. Kayed, A. Kozak, B. Edmonds, T.M. McIntire, S. Milton, M. Cahalan, C.G. Glabe, J.E. Hall, Soluble amyloid oligomers increase lipid bilayer conductance by increasing the dielectric constant of the hydrocarbon core, Biophysical Journal 86 (2004) 382A-382A.
[5] S.M. Butterfield, H.A. Lashuel, Amyloidogenic protein membrane interactions: mechanistic insight from model systems, Angewandte Chemie International Edition 49 (2010) 5628–5654.
[6] D.M. Hartley, D.M. Walsh, C.P. Ye, T. Diehl, S. Vasquez, P.M. Vassilev, D.B. Teplow, D.J. Selkoe, Protofibrillar intermediates of amyloid β-protein induce acute electrophysiological changes and progressive neurotoxicity in cortical neurons, Journal of Neuroscience 19 (1999) 8876–8884.
[7] D.M. Walsh, I. Klyubin, J.V. Fadeeva, W.K. Cullen, R. Anwyl, M.S. Wolfe, M.J. Rowan, D.J. Selkoe, Naturally secreted oligomers of amyloid beta protein potently inhibit hippocampal long-term potentiation in vivo, Nature 416 (2002) 535–539.
[8] J. McLaurin, A. Chakrabartty, Membrane disruption by Alzheimer β-amyloid peptides mediated through specific binding to either phospholipids or gangliosides. Implications for neurotoxicity, Journal of Biological Chemistry 271 (1996) 26482–26489.
[9] C.M. Yip, J. McLaurin, Amyloid-beta peptide assembly: a critical step in fibrillogenesis and membrane disruption, Biophysical Journal 80 (2001) 1359–1371.
[10] A. Demuro, E. Mina, R. Kayed, S.C. Milton, I. Parker, C.G. Glabe, Calcium dysregulation and membrane disruption as a ubiquitous neurotoxic mechanism of soluble amyloid oligomers, Journal of Biological Chemistry 280 (2005) 17294–17300.
[11] S. Dante, T. Hauss, R. Steitz, C. Canale, N.A. Dencher, Nanoscale structural and mechanical effects of beta-amyloid (1–42) on polymer cushioned membranes: a combined study by neutron reflectometry and AFM force spectroscopy, BBA — Biomembranes 1808 (2011) 2646–2655.
[12] A. Relini, O. Cavalleri, R. Rolandi, A. Gliozzi, The two-fold aspect of the interplay of amyloidogenic proteins with lipid membranes, Chemistry and Physics of Lipids 158 (2009) 1–9.
[13] R. Richter, A. Mukhopadhyay, A. Brisson, Pathways of lipid vesicle deposition on solid surfaces: a combined QCM-D and AFM study, Biophysical Journal 85 (2003) 3035–3047.
[14] C. Rossi, J. Chopineau, Biomimetic tethered lipid membranes designed for membrane–protein interaction studies, European Biophysics Journal 36 (2007) 955–965.
[15] C. Canale, M. Jacono, A. Diaspro, S. Dante, Force spectroscopy as a tool to investigate solid supported lipid membranes, Microscopy Research and Technique 73 (2010) 965–972.
[16] M.P. Mingeot-Leclercq, M. Deleu, R. Brasseur, Y.F. Dufrene, Atomic force microscopy of supported lipid bilayers, Nature Protocols 3 (2008) 1654–1659.
[17] S. Dante, T. Hauss, A. Brandt, N.A. Dencher, Membrane fusogenic activity of the Alzheimer's peptide A beta(1–42) demonstrated by small-angle neutron scattering, Journal of Molecular Biology 376 (2008) 393–404.
[18] S. Dante, T. Hauss, N.A. Dencher, Beta-amyloid 25 to 35 is intercalated in anionic and zwitterionic lipid membranes to different extents, Biophysical Journal 83 (2002) 2610–2616.
[19] Y. Fezoui, D.M. Hartley, J.D. Harper, R. Khurana, D.M. Walsh, M.M. Condron, D.J. Selkoe, P.T. Lansbury, A.L. Fink, D.B. Teplow, An improved method of preparing the amyloid beta-protein for fibrillogenesis and neurotoxicity experiments, Amyloid 7 (2000) 166–178.
[20] H. Edelhoch, Spectroscopic determination of tryptophan and tyrosine in proteins, Biochemistry 6 (1967) 1948–1954.
[21] J.L. Hutter, J. Bechhoefer, Calibration of atomic-force microscopy tips, The Review of Scientific Instruments 64 (1993) 1868–1873.
[22] R. Carrotta, C. Canale, A. Diaspro, A. Trapani, P.L. San Blagio, D. Bulone, Inhibiting effect of alpha(s1)-casein on Abeta(1–40) fibrillogenesis, Biochimica et Biophysica Acta 1820 (2012) 124–132.
[23] C. Canale, B. Torre, D. Ricci, P.C. Braga, Recognizing and avoiding artifacts in atomic force microscopy imaging, Methods in Molecular Biology 736 (2011) 31–43.
[24] J. McLaurin, C.M. Yip, Modulation of A beta fibrillogenesis on the bilayer surface, Amyloid - Journal of Protein Folding Disorders 8 (2001) 138–139.
[25] C.M. Pfefferkorn, Z. Jiang, J.C. Lee, Biophysics of alpha-synuclein membrane interactions, Biochimica et Biophysica Acta 1818 (2012) 162–171.
[26] J.D. Green, L. Kreplak, C. Goldsbury, X.L. Blatter, M. Stolz, G.S. Cooper, A. Seelig, J. Kist-Ler, U. Aebi, Atomic force microscopy reveals defects within mica supported lipid bilayers induced by the amyloidogenic human amylin peptide, Journal of Molecular Biology 342 (2004) 877–887.
[27] S. Garcia-Manyes, L. Redondo-Morata, G. Oncins, F. Sanz, Nanomechanics of lipid bilayers: heads or tails? Journal of the American Chemical Society 132 (2010) 12874–12886.
[28] W.E. Muller, S. Koch, A. Eckert, H. Hartmann, K. Scheuer, Beta-amyloid peptide decreases membrane fluidity, Brain Research 674 (1995) 133–136.